



ARL-TR-8224 • Nov 2017



Validating a Finite Element Model of a Structure Subjected to Mine Blast with Experimental Modal Analysis

**by Douglas Howle, Dmitriy Kraytermann, Justin E Pritchett,
and Ryan Sorenson**

Approved for public release; distribution is unlimited.

NOTICES

Disclaimers

The findings in this report are not to be construed as an official Department of the Army position unless so designated by other authorized documents.

Citation of manufacturer's or trade names does not constitute an official endorsement or approval of the use thereof.

Destroy this report when it is no longer needed. Do not return it to the originator.



Validating a Finite Element Model of a Structure Subjected to Mine Blast with Experimental Modal Analysis

by Douglas Howle

Survivability/Lethality Analysis Directorate, ARL

Dmitriy Krayterman

Weapons and Materials Research Directorate, ARL

Justin E Pritchett and Ryan Sorenson

Oak Ridge Institute for Science and Education

REPORT DOCUMENTATION PAGE				Form Approved OMB No. 0704-0188	
<p>Public reporting burden for this collection of information is estimated to average 1 hour per response, including the time for reviewing instructions, searching existing data sources, gathering and maintaining the data needed, and completing and reviewing the collection information. Send comments regarding this burden estimate or any other aspect of this collection of information, including suggestions for reducing the burden, to Department of Defense, Washington Headquarters Services, Directorate for Information Operations and Reports (0704-0188), 1215 Jefferson Davis Highway, Suite 1204, Arlington, VA 22202-4302. Respondents should be aware that notwithstanding any other provision of law, no person shall be subject to any penalty for failing to comply with a collection of information if it does not display a currently valid OMB control number.</p> <p>PLEASE DO NOT RETURN YOUR FORM TO THE ABOVE ADDRESS.</p>					
1. REPORT DATE (DD-MM-YYYY) November 2017		2. REPORT TYPE Technical Report		3. DATES COVERED (From - To) October 2012 – September 2013	
4. TITLE AND SUBTITLE Validating a Finite Element Model of a Structure Subjected to Mine Blast with Experimental Modal Analysis				5a. CONTRACT NUMBER	
				5b. GRANT NUMBER	
				5c. PROGRAM ELEMENT NUMBER	
6. AUTHOR(S) Douglas Howle, Dmitriy Krayterman, Justin E Pritchett, and Ryan Sorenson				5d. PROJECT NUMBER	
				5e. TASK NUMBER	
				5f. WORK UNIT NUMBER	
7. PERFORMING ORGANIZATION NAME(S) AND ADDRESS(ES) US Army Research Laboratory ATTN: RDRL-SLB-E Aberdeen Proving Ground, MD 21005				8. PERFORMING ORGANIZATION REPORT NUMBER ARL-TR-8224	
9. SPONSORING/MONITORING AGENCY NAME(S) AND ADDRESS(ES)				10. SPONSOR/MONITOR'S ACRONYM(S)	
				11. SPONSOR/MONITOR'S REPORT NUMBER(S)	
12. DISTRIBUTION/AVAILABILITY STATEMENT Approved for public release; distribution is unlimited.					
13. SUPPLEMENTARY NOTES					
14. ABSTRACT <p>The Under-body Blast Methodology (UBM) for the Test and Evaluation (T&E) program was established to provide a capability for the US Army Test and Evaluation Command to assess the vulnerability of vehicles to under-body blast. Finite element (FE) models are part of the current UBM for T&E methodology and must be validated. The UBM for the T&E program has completed efforts to validate soil models but not structural dynamics models. Modal testing of a V-hull structure was performed. The modal test setup, execution, and results obtained are presented. Changes made to the existing FE model of the structure as part of the validation process are presented. The effect of the model validation on the shock response of the structure during a mine blast simulation was quantified using a correlation and analysis (CORA) tool. In general, all models—whether validated or nonvalidated—provided acceptable predictions of structural response.</p>					
15. SUBJECT TERMS Under-body Blast Methodology (UBM), mine blast, finite element analysis, LS-DYNA, modal testing, model updating					
16. SECURITY CLASSIFICATION OF:			17. LIMITATION OF ABSTRACT UU	18. NUMBER OF PAGES 42	19a. NAME OF RESPONSIBLE PERSON Douglas Howle
a. REPORT Unclassified	b. ABSTRACT Unclassified	c. THIS PAGE Unclassified			19b. TELEPHONE NUMBER (Include area code) 410-278-5738

Contents

List of Figures	iv
List of Tables	v
1. Introduction and Background	1
2. Issue	2
3. Objectives	2
4. Design of V-hull Structure	2
5. Experimental Modal Analysis	3
6. Finite Element Model Updating	7
7. ConWep Blast Analysis	15
8. ALE Blast Analysis	18
9. Conclusions	24
10. References	25
Appendix. Detailed CORA Reports	27
List of Symbols, Abbreviations, and Acronyms	33
Distribution List	34

List of Figures

Fig. 1	Overall dimensions of the V-hull structure and initial conditions for test. The angle theta is equal to 20 degrees.....	3
Fig. 2	As seen in photos from a range test, the V-hull has tabs on the sides of it to support the structure on the range.....	3
Fig. 3	V-hull ground isolation, grid, and accelerometer mounting locations	4
Fig. 4	V-hull accelerometer location on flat plate.....	4
Fig. 5	Roving hammer test	5
Fig. 6	V-hull experimental modal model	6
Fig. 7	Curve fitting to extract modal parameters	6
Fig. 8	Experimental modal assurance criteria for first 5 modes.....	7
Fig. 9	Baseline FE Model of the V-hull	8
Fig. 10	Mode shape comparison between the baseline FE model and the experiment.....	10
Fig. 11	Improvements to shape and dimensions of the FE model	12
Fig. 12	Improvements to mesh and connections of the FE model	12
Fig. 13	Mode shape comparison between the updated FE model and the experiment.....	14
Fig. 14	Nonvalidated model prediction vs. test.....	16
Fig. 15	Validated model prediction vs. test.....	17
Fig. 16	ALE representation of the air, soil, and mine with the validated structural model	19
Fig. 17	Band of displacements derived from test data	20
Fig. 18	Band of displacements derived from test data and model-predicted displacement using the nonvalidated structural model	21
Fig. 19	Band of displacements derived from test data and model-predicted displacement using the validated structural model	22
Fig. 20	Band of displacements derived from test data and model-predicted displacement using the validated structural model. The data from the structural model was filtered with an SAE filter at 300 Hz.	23

List of Tables

Table 1	Experimental modal model coefficients	6
Table 2	Baseline FE model vs. experimental natural frequency correlation summary.....	9
Table 3	Analysis vs. experimental modal frequency summary	13
Table 4	Comparison of CORA scores for all model predictions	23

INTENTIONALLY LEFT BLANK.

1. Introduction and Background

The Under-body Blast Methodology (UBM) for the Test and Evaluation (T&E) program was established to provide a capability for the US Army Test and Evaluation Command (ATEC) to assess the vulnerability of vehicles to under-body blast. In order for ATEC to use the capability, the methodology and any models used must go through a formal verification, validation, and accreditation (VV&A) process.^{1,2} The organization leading the effort to develop this new capability is the US Army Research Laboratory (ARL) Survivability/Lethality Analysis Directorate (SLAD). Other organizations involved in the UBM for T&E program are the ARL Weapons and Materials Research Directorate (WMRD), the Army Material Systems Analysis Activity (AMSAA), the Tank Automotive Research, Development and Engineering Center (TARDEC) and the US Army Engineer Research and Development Center (ERDC).

Finite element (FE) models are part of the current UBM for T&E methodology and must be validated. LS-DYNA is used by the ARL/SLAD to model the structure subjected to mine blast as well as the soil and explosives that make up the threat. Similar techniques have been used by others.³⁻⁶ Previously, the ARL/WMRD validated soil models for arbitrary Lagrangian-Eulerian (ALE) based simulations.⁷ As part of the UBM program, experiments were performed to obtain data to validate simulations of structural response.⁸ In the experiments, stereo-digital image correlation (SDIC) was used to record the shock response of a V-hull structure during a series of blast experiments. Simulations of these experiments were also performed⁹ using the validated soil model to verify that the impulse imparted to the V-hull from the soil and explosive were correct and that the structural response of the hull reasonably matched that recorded by the SDIC cameras.

Structural model validation is often employed by structural dynamists to correlate experimental measurements with numerical solutions. ARL has used modal analysis to validate structural models of vehicles subjected to ballistic shock.¹⁰⁻¹² Modal analysis is a technique used to study the response of linear structures. For a mine blast problem in which there aren't many nonlinear considerations, such as structural yielding, it may be beneficial to validate the modal response of the V-hull FE model to have confidence that the overall mass and stiffness of the physical structure is captured by the FE model.

2. Issue

The UBM for T&E program has completed efforts to validate soil models but not structural dynamics models. Furthermore, it has not been determined if modal-based validation of a structural model is necessary to obtain the best possible structural response predictions.

3. Objectives

The objectives of this report are to:

1. Describe the setup, execution, and results obtained from modal tests of the V-hull structure.
2. Document changes made to the existing FE model of the structure as part of the validation process.
3. Quantify the effect of the model validation on the shock response of the structure during a mine blast simulation.

4. Design of V-hull Structure

The V-hull structure was originally constructed for a series of tests that were conducted at Aberdeen Proving Ground (APG) to obtain validation data for the UBM for T&E modeling and simulation capability. Details regarding the test conditions and results can be obtained in other reports.¹³ The V-hull was considered a good candidate for this investigation because of the existing test data, the simplicity of the structure's design, and the desire for model predictions to compare well to the test data. The V-hull was constructed from A-36 steel and has a mass of approximately 227 kg. The overall dimensions of the structure are shown in Fig. 1. All of the V-hull's parts were 25.4 mm in thickness with the exception of the top plate, which is only 12.7 mm thick. The top plate is colored blue in Fig. 2 and the rest of the parts are colored red. The thickness of the top plate was designed using finite element modeling of the tests conducted before the tests were completed. The thickness was chosen so that the deflections of the top plate would be large enough to be easily recorded by instrumentation but not so large that it came into contact with any internal supports.

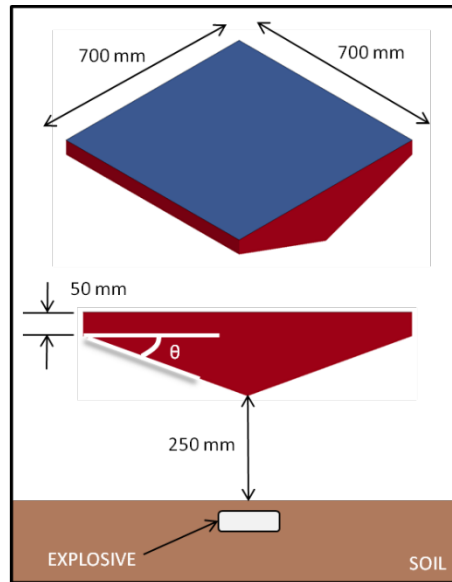


Fig. 1 Overall dimensions of the V-hull structure and initial conditions for test. The angle theta is equal to 20 degrees.

In order to position the structure relative to the ground during range testing, 4 steel tabs were welded to the V-hull. These tabs and the frame rails on which the tabs rest can be seen in Fig. 2.



Fig. 2 As seen in photos from a range test, the V-hull has tabs on the sides of it to support the structure on the range.

The range testing was successfully completed and the V-hull structure was placed into storage while new simulations of the tests were completed. During this time the decision was made to perform modal testing on the structure. The V-hull was transferred from APG to the Adelphi Laboratory Center (ALC).

5. Experimental Modal Analysis

After being transported to a lab at ALC, modal testing began. The V-hull structure was supported on 4 air mounts to provide a free-free boundary condition. The air mounts were pressurized to 5 psi, resulting in rigid-body modes outside the

frequency bandwidth of interest. Arrays of test points were created on each surface in a 2 inch \times 2 inch grid pattern. The grid pattern was recessed inward from each edge 2 inches to avoid measurements on the welded edges. The structure was instrumented with 3 accelerometers: 1 on the “V” plate, 1 on the flat plate, and 1 on the triangular side. The accelerometers were secured to the structure via mounting wax and were placed on test point locations that were predicted to not lie on a nodal line or line where no displacement occurs (Figs. 3 and 4).

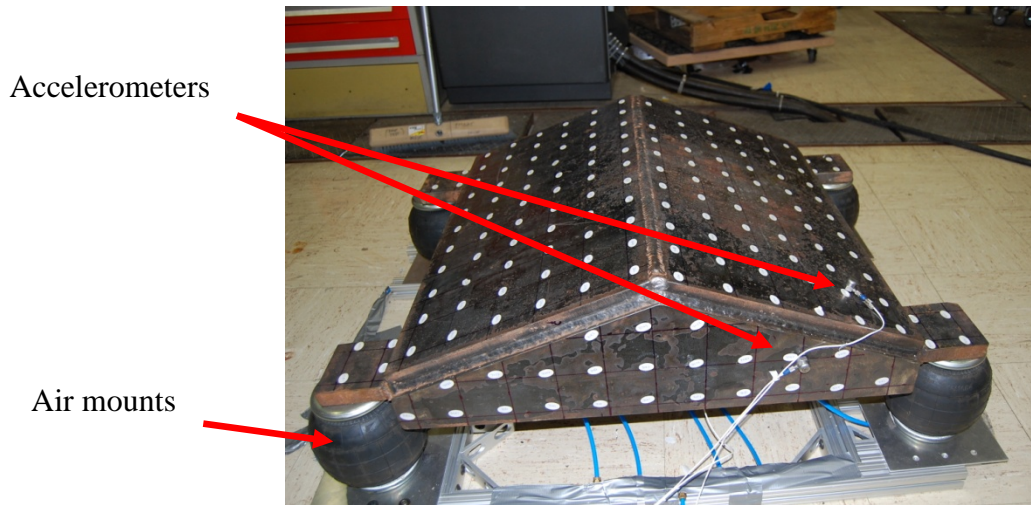


Fig. 3 V-hull ground isolation, grid, and accelerometer mounting locations

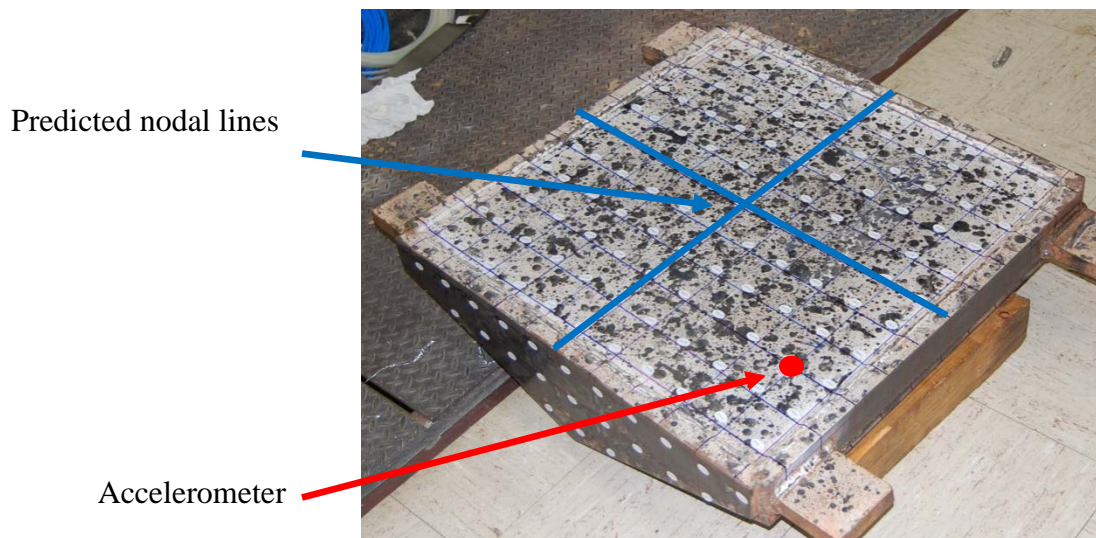


Fig. 4 V-hull accelerometer location on flat plate

Roving hammer tests were performed on all 335 test points comprised from all surfaces (Fig. 5). The X, Y, and Z coordinates for each point, established from a datum origin, were imported into Spectral Dynamics STAR7 (San Jose, CA) modal analysis software and the experimental modal model was constructed (Fig. 6). The force input from the hammer and the response from all 3 accelerometers were applied to each node in the modal model. The responses from the 3 accelerometers were averaged and curve fitting techniques were used to extract the mode shapes, modal frequencies, and damping coefficients (Fig. 7). Data obtained from the curve fitting analysis is summarized in Table 1.



Fig. 5 Roving hammer test

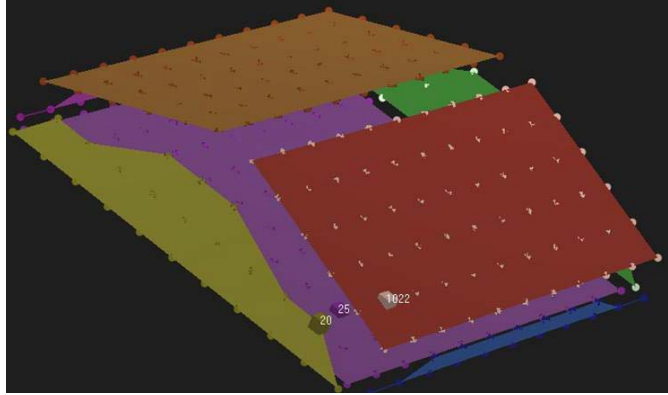


Fig. 6 V-hull experimental modal model

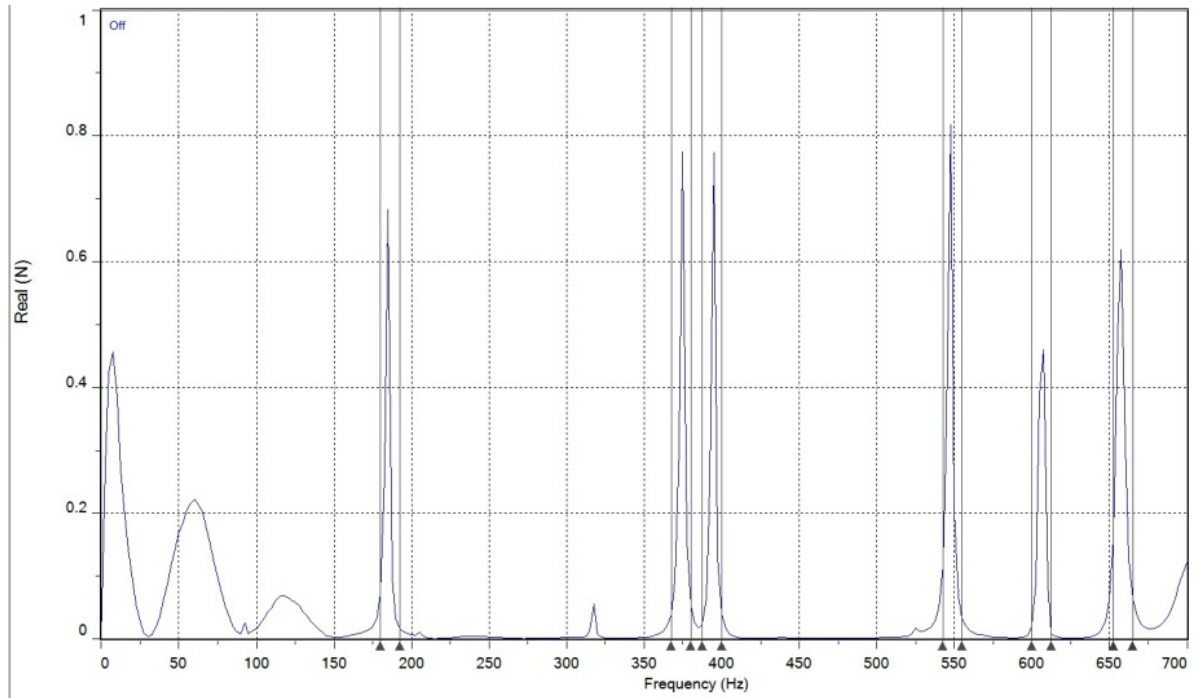


Fig. 7 Curve fitting to extract modal parameters

Table 1 Experimental modal model coefficients

	Frequency (Hz)	Damping (Hz)	Damping (%)	Compensated (%)	Magnitude	Phase
Mode 1	182.60	1.99	1.09	1.09	2.7845e-001	-6.60
Mode 2	371.38	2.03	0.55	0.55	2.6489e+000	-3.87
Mode 3	392.78	2.14	0.55	0.55	1.1244e+000	-5.36
Mode 4	544.46	2.01	0.37	0.37	9.4396e+000	175.75
Mode 5	603.78	4.98	0.82	0.82	6.0932e-001	131.01

The modal assurance criteria (MAC) numbers calculated using the experimental data are shown in Fig. 8. The computed MAC numbers indicate that good measurements were recorded during the modal test.

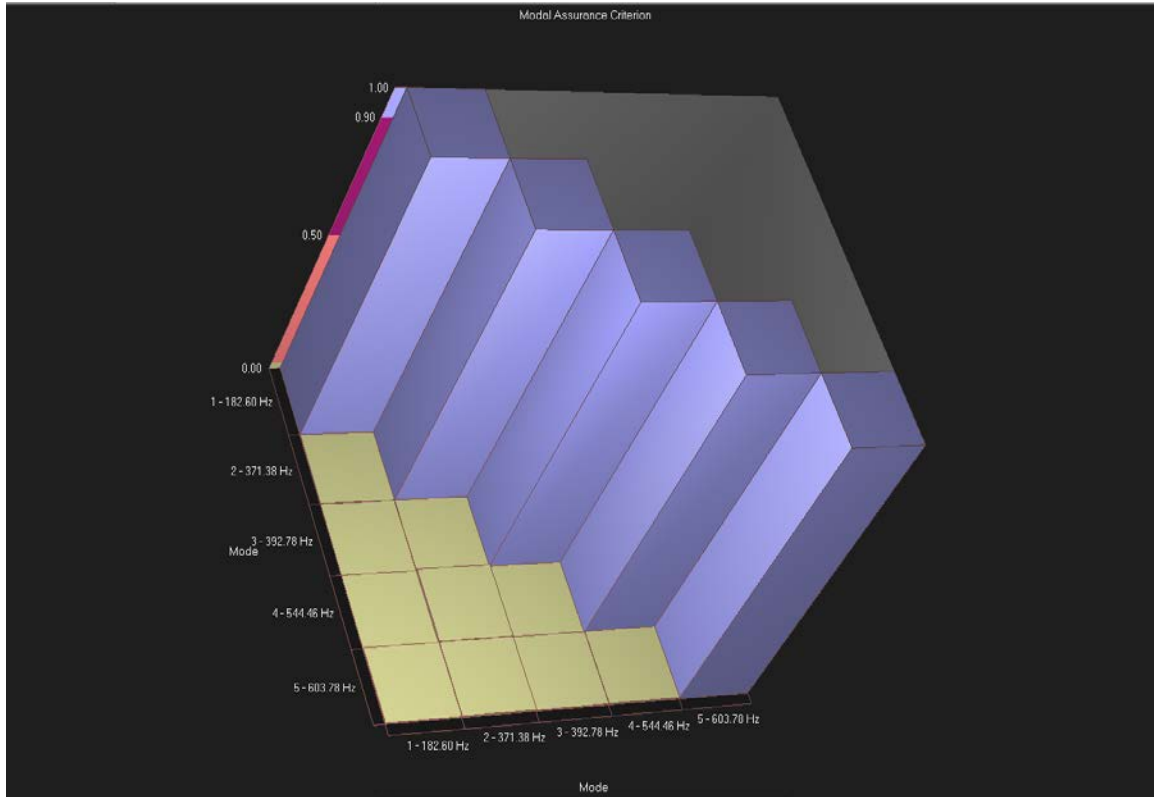


Fig. 8 Experimental modal assurance criteria for first 5 modes

After completing the modal tests, attention turned toward updating the finite element model so that the mode shapes and natural frequencies obtained from the experimental modal analysis match those calculated from the model.

6. Finite Element Model Updating

The baseline (or original) FE Model (Fig. 9) of the V-hull created by ARL/SLAD contains 45,748 8-noded solid elements approximately 10 mm in length. A simplified version of the Johnson Cook material card in LS-DYNA was used to model the A36 steel from which the structure was built. All relevant Johnson Cook parameters were obtained from literature.¹⁴ The width and length of the model is

0.7 m. All parts of the structure are 25.4 mm thick except for the top plate, which is 12.7 mm thick.

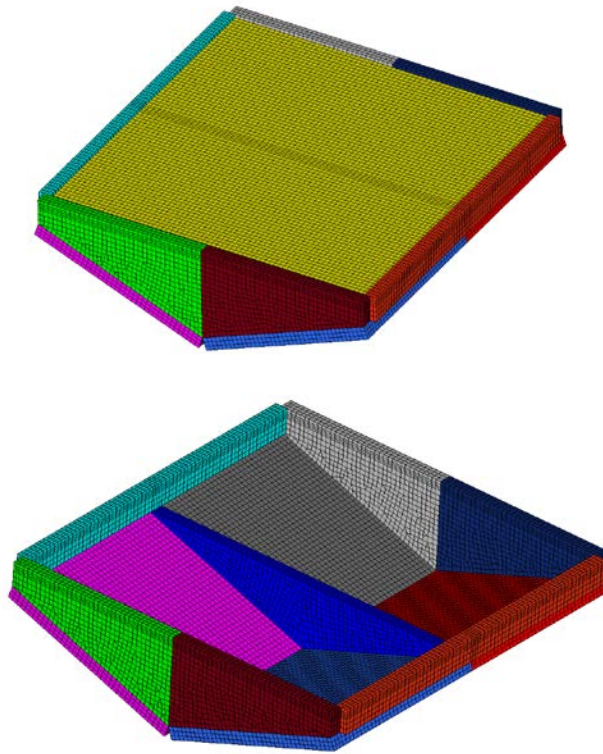


Fig. 9 Baseline FE Model of the V-hull

Modal analysis was performed on the baseline model using the Livermore Software Technology Corporation LS-DYNA ls971d R5.1.0 implicit eigenvalue solver to obtain the mode shapes and natural frequencies of the modeled structure. The boundary conditions in the model were assumed to be “free-free”, meaning that no physical constraints were applied.

1. Initial assessment of baseline model

To assess the accuracy of the baseline model, the first 5 natural frequencies and mode shapes were extracted from the analysis and compared to the experimental results. The results are summarized in Table 2.

Table 2 Baseline FE model vs. experimental natural frequency correlation summary

	Experiment mode frequency (Hz)	Baseline FE model mode frequency (Hz)	Percent error
Mode 1	184.4	223.6	21.2
Mode 2	375.4	386.7	3.0
Mode 3	394.7	460.6	16.7
Mode 4	547.1	600.8	9.8
Mode 5	606.1	603.5	-0.4

The mode shape comparison between the baseline model and the experiment is shown in Fig. 10.

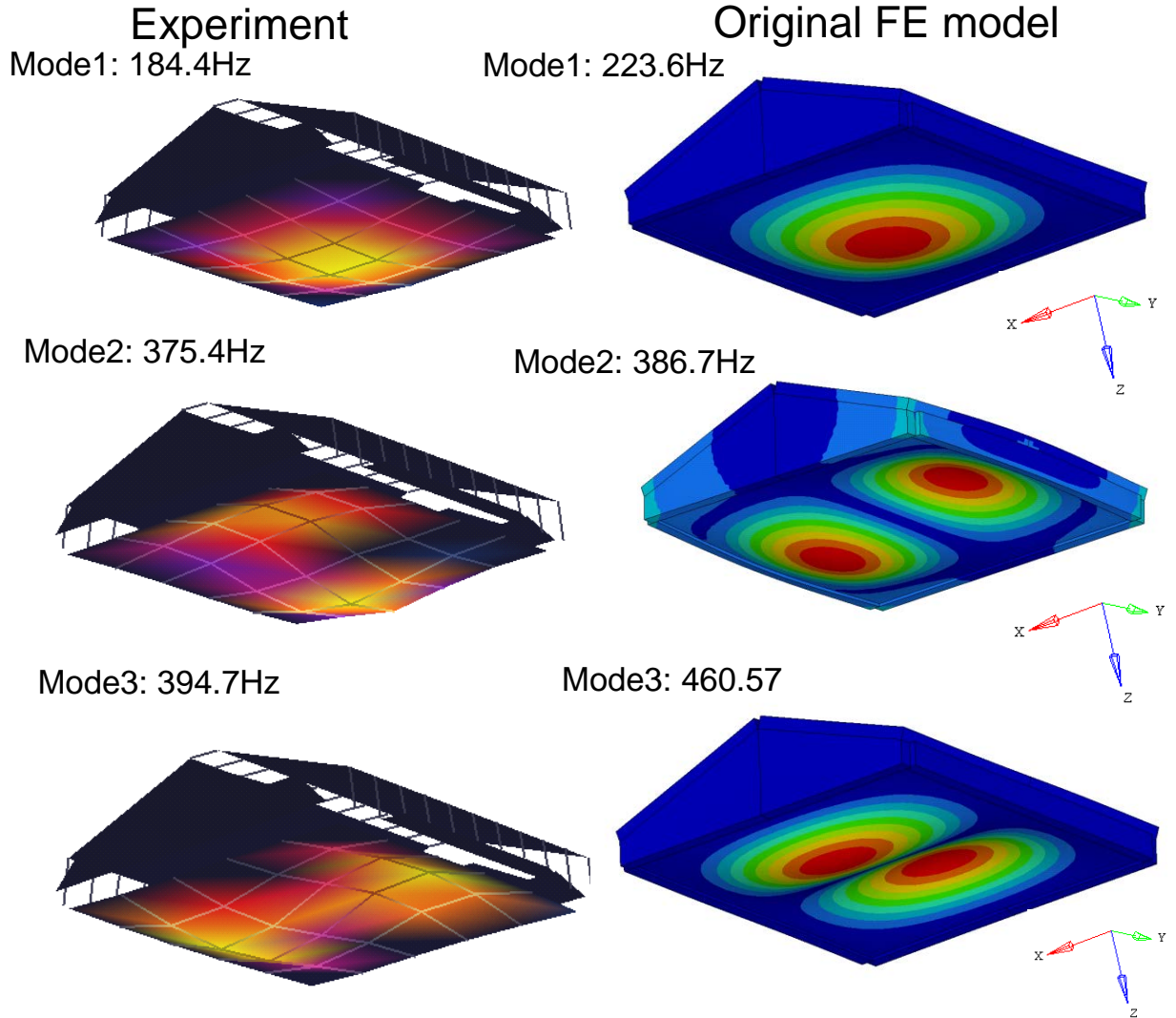


Fig. 10 Mode shape comparison between the baseline FE model and the experiment

The natural frequency predicted by the FE model for the first mode is approximately 21% higher than that observed in the experiment. Modes 2 and 3 show acceptable natural frequency correlation, but the shapes are rotated 90° about vertical (Z) axis. In the experiments, the structural responses obtained from the mine blast experiment appear to be dominated by the first mode of vibration. Visual inspections of the recorded structural responses and the associated fast Fourier transforms corroborate this statement.⁹ Therefore, the first mode is considered the most important metric for accurate structural response prediction. It is important to reduce the model prediction error as much as possible to match the experiment. After comparing the FE model to the physical test asset, the model was updated by refining the geometry and adjusting some material properties.

It is hoped that updating the geometry and material properties would help the natural frequencies and mode shapes to match better.

2. The updated FEA model

The natural frequency, f_n , of an undamped spring system can be found using the following formula:

$$f_n = \frac{1}{2\pi} \sqrt{\frac{k}{m}}$$

Where:

f_n = natural frequency in Hertz (cycles/second)

k = stiffness of the spring (N/m)

m = mass (kg)

According to the formula above, the proper stiffness (k) and mass (m) of the structure are essential for accurate natural frequency calculation. Therefore, the FE model updates should be made to closely match the experimental unit's shape, dimensions, connections, and material properties to accurately represent the stiffness and mass of the unit. Simplifying assumptions made in the construction of the baseline FE model and uncertainty in material properties are the most likely causes of any discrepancy between the model response of the baseline FE model and the actual structure. ARL/WMRD completed many model modifications during the correlation process. The major model updates and modifications are presented next.

Model modification #1 (Fig. 11) – updates to shape and dimensions of the model to better represent the mass and stiffness of the test article

- Plates were repositioned to better reflect actual measured dimensions and relative positions of parts in the welded V-hull structure
- Welds between plates and support tabs were added

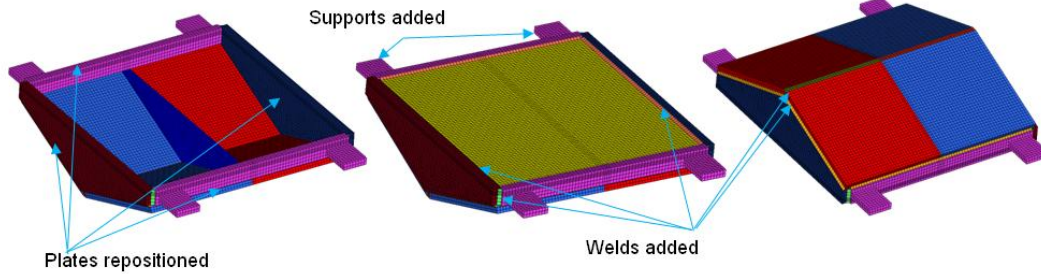


Fig. 11 Improvements to shape and dimensions of the FE model

Model modification #2 (Fig. 12) – updates to mesh and connections of the model to better represent the stiffness of the test article

- Top plate was remeshed to add extra element layer
- Top plate edge was partially detached from the side walls to closely represent welded connection
- Elements were added to represent the welded part of the structure

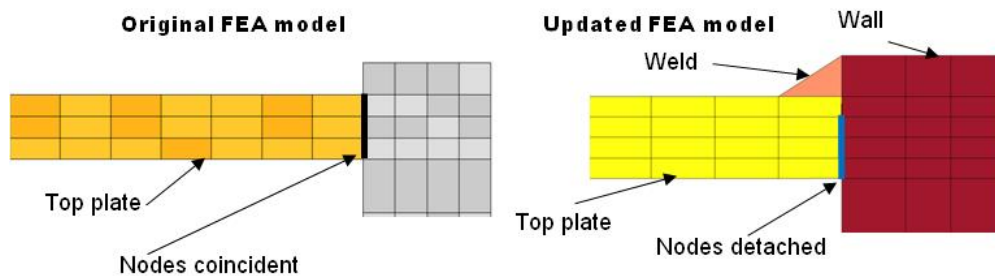


Fig. 12 Improvements to mesh and connections of the FE model

Model modification #3 – minor updates to the material density of the model to better match the actual mass of the test article

Total Mass:	Test article	~500 lb (227 kg)
	FEA model	225 kg

3. Updated FEA model correlation results

The modal analysis identical to that of the baseline model was performed on the updated FE model and the first 4 natural frequencies and mode shapes were extracted. The natural frequency results are summarized in Table 3 and mode shape correlation is shown in Fig. 13.

Table 3 Analysis vs. experimental modal frequency summary

Frequency (hz)	Experiment	Original FE model	% error	Updated FE model	% error
Mode 1	184.4	223.6	21.3	185.4	0.5
Mode 2	375.4	386.7	3.0	366.4	-2.4
Mode 3	394.7	460.6	16.7	382.6	-3.1
Mode 4	547.1	600.8	9.8	531.8	-2.8

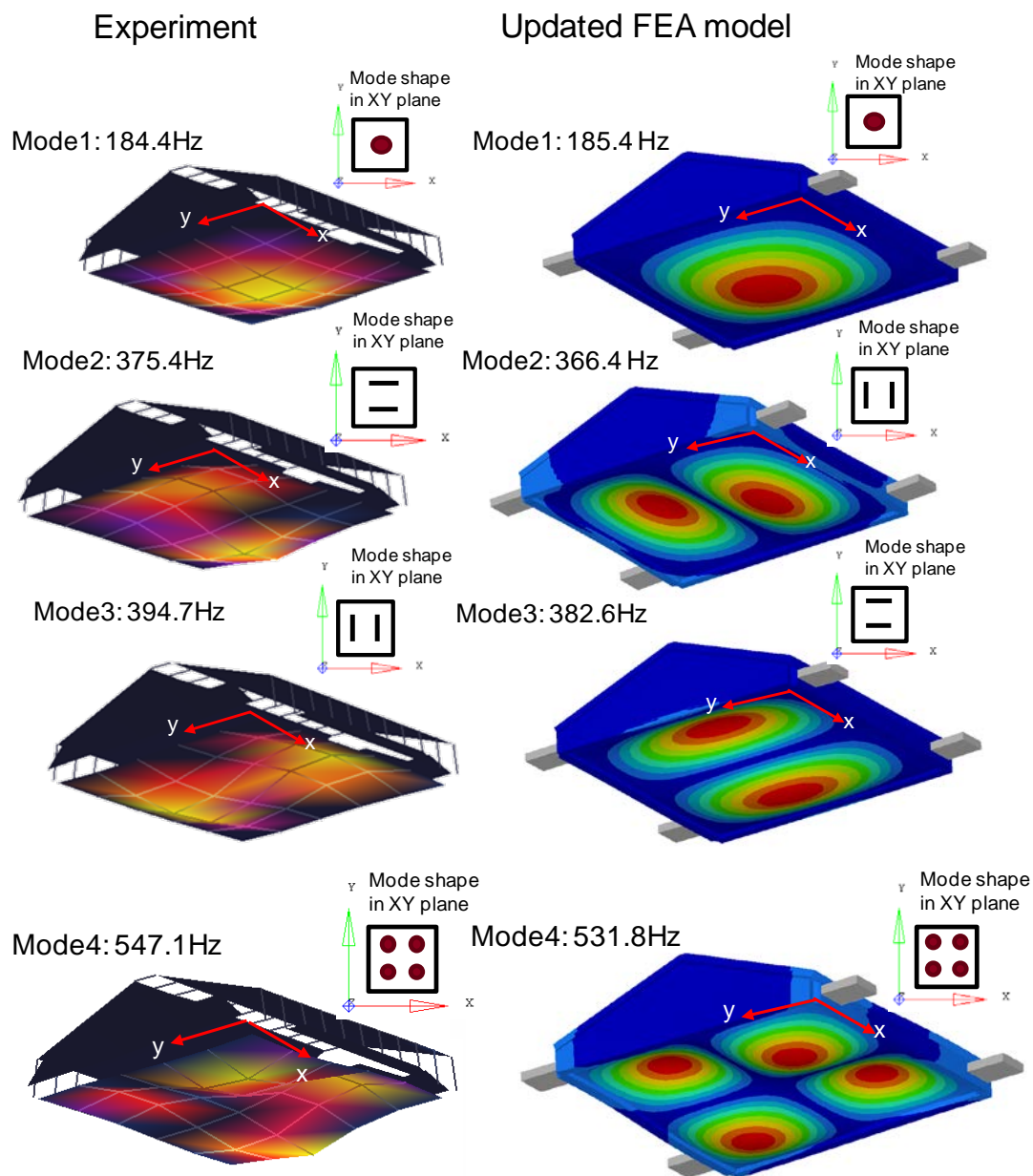


Fig. 13 Mode shape comparison between the updated FE model and the experiment

The following bullet points summarize some basic observations and conclusions obtained during the model update exercise:

- All modes extracted (Mode 1 through Mode 4) occur in the thin plate—by far the least stiff part of the V-hull structure
- The updated FEA model matches experimental natural frequencies within approximately 3% for the first 4 natural frequencies. However, the mode shapes for the 2nd and 3rd mode seem to be rotated 90° about the vertical axis of the model. This may be due to modeling or computational inaccuracy and/or experimental data processing error. Ideally, for the thin, perfectly square plate that is fully constrained at all edges, the natural frequencies are supposed to be identical. In reality, as demonstrated in the experiment and the model, the difference in natural frequencies is approximately 20 Hz.
- It is very important that the FE model accurately represents welded connections so that parts are not over constrained. Modeling welds and partially detaching the plate's edge nodes was the **key model update** technique that brought natural frequencies predicted by the model very close to the natural frequencies observed in the experiment. Although the FE model matches the experimental results reasonably well, it is recommended to cut the V-hull to inspect the structure's interior and welds to further update the FE model and improve model correlation with experimental results (mode shapes).

Having completed the model updating process, the original FE model is considered validated from a modal perspective. Next, attention is turned toward performing mine blast simulations to determine the effect of model updating on the predicted structural responses under blast conditions. Two types of loading approaches will be used: ConWep and ALE.

7. ConWep Blast Analysis

ConWep refers to a collection of conventional weapons effects calculations based on the equations and curves of TM-5-855-1, *Design and Analysis of Hardened Structures to Conventional Weapons Effects*.^{15,16} Specifically, in this analysis we are focusing on the empirical air blast equations from ConWep, which were encoded within LS-DYNA. For a given amount of TNT explosive and a charge location, the pressures on a target can be calculated in LS-DYNA. Even though the ConWep air-blast equations apply to free air blasts and not buried blasts, this approach is sometimes used to simulate mine blast because of its ease and reduced computation time compared to other simulation techniques.^{17,18} To account for the

impulse to a target from the soil and confinement of the blast, scaling factors can be applied to the predicted pressures to obtain a realistic total impulse.

Since ConWep can be scaled to match a specific impulse, a scale factor was chosen for both models such that the impulse applied to the target was approximately 1107 N-s. The factor for each structural model was slightly different. The factor for the nonvalidated model was 2.67. The factor for the validated model was 2.76. Impulses from the models were calculated from the total momentum change of all the parts in the model.

Time histories of displacement from the center of the nonvalidated hull model and test are plotted in Fig. 14. Time histories of displacement from the center of the validated hull model and test are plotted in Fig. 15. The timing of the minimum values for each graph did not compare well between model and test so the time histories from the models were shifted slightly in time. The time at which the minimum displacements occur match exactly because of this time shift. None of the data from either the model or the test was filtered before generating the plots in Figs. 14 and 15.

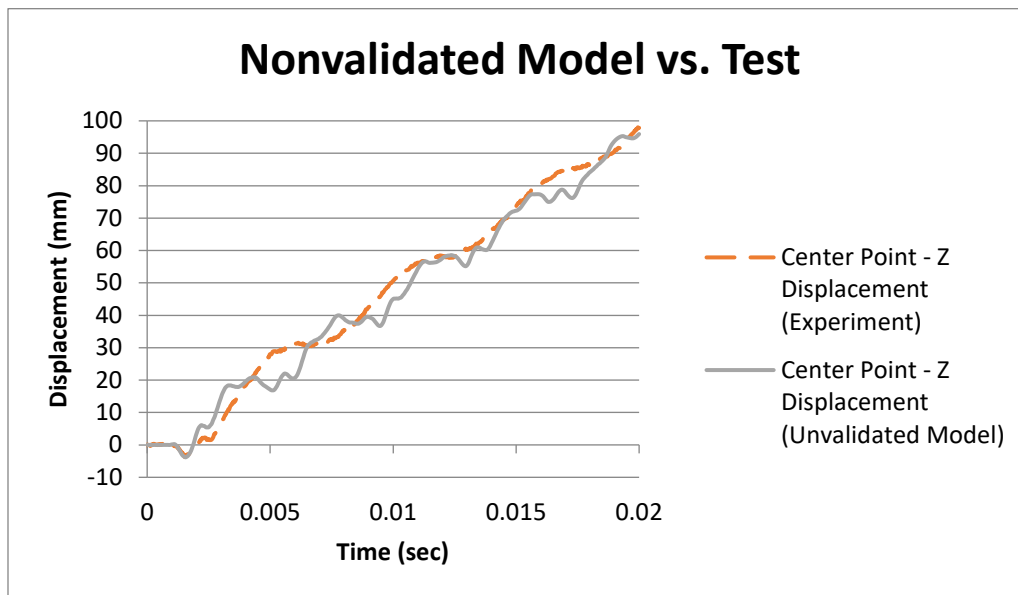


Fig. 14 Nonvalidated model prediction vs. test

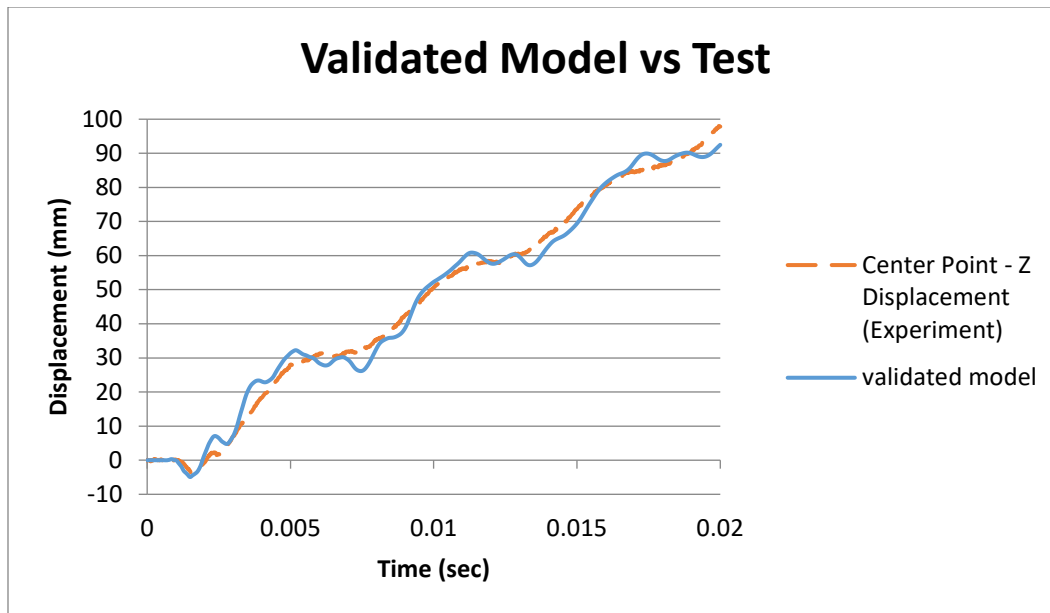


Fig. 15 Validated model prediction vs. test

A visual inspection of Figs. 14 and 15 indicates that the time history from the validated model is more comparable to the experimental data than the time history from the nonvalidated model. Ideally the time histories from the validated model and experiment would be identical but this is not the case. The modeled target appears to respond at a much larger range of frequencies than the experimental target. This observation could be a result of differences in the loading of each target, shortcomings in how the experimental data is processed, or some other problem such as material models. For example, previous modeling efforts have shown⁹ how uncertainty in the constitutive relations and loading model will affect the response of a structure subjected to mine blast. Any discrepancy between the time histories in Fig. 15 could be a result of those uncertainties. However, the cause of the difference between the model and test responses may not be limited to those 2 items.

To quantify the effect of model validation on the FE model predictions, a correlation and analysis (CORA) tool was exercised. The re tool compares signals using 2 approaches. The first approach, the corridor method, uses statistics derived from the data to apply inner and outer limits or corridors to the experimental data. The simulation data is compared to the experimental data's corridors and rated between 0 and 1. A CORA value of 1 represents a very good rating—the simulation data tracks the experimental data very well. A CORA value of 0 is a poor rating—there is no correlation between the experimental and simulation data. Ratings between 0 and 1 are calculated based on where the model prediction falls within the corridors. The second approach used by the CORA tool is the cross-correlation

method. The cross-correlation method compares aspects such as magnitude and phase between the curves to establish another comparison rating between 0 and 1. The final CORA rating for the comparison is an average of the results from each CORA approach.¹⁹ When the CORA tool was used to compare the prediction of displacement from the nonvalidated structural model to the test data, a final rating of 0.865 was obtained. When the CORA tool was used to compare the prediction of displacement from the validated structural model to the test data, a final rating of 0.947 was obtained. Generally, a CORA score greater than 0.7 is considered to mean there is favorable agreement between the model-predicted response and recorded test data.²⁰ The CORA rating for the validated FE model is higher than the rating for the nonvalidated model, suggesting that modal validation of the model improved the comparison to the test results. Regardless of the improvement both are rated greater than 0.7. The FE model predictions appear to be representative of the sample of test data points used for comparison.

8. ALE Blast Analysis

An ALE model was constructed to validate the ability of an ALE loading to predict impulse. It was demonstrated previously,⁹ that the loading model used can affect the structural response prediction. Specifically for the sandbox V-hull, the ALE loading approach predicted much smaller structural displacements than the ConWep approach. Physically, an ALE loading approach is more realistic than ConWep. The ALE approach can simulate the soil and explosive as well as the interaction of those two with the target and each other. ConWep was developed as an air blast model and fails to account for soil and confinement of the charge. Figure 16 displays the ALE representation of the loading as well as the validated structural model.

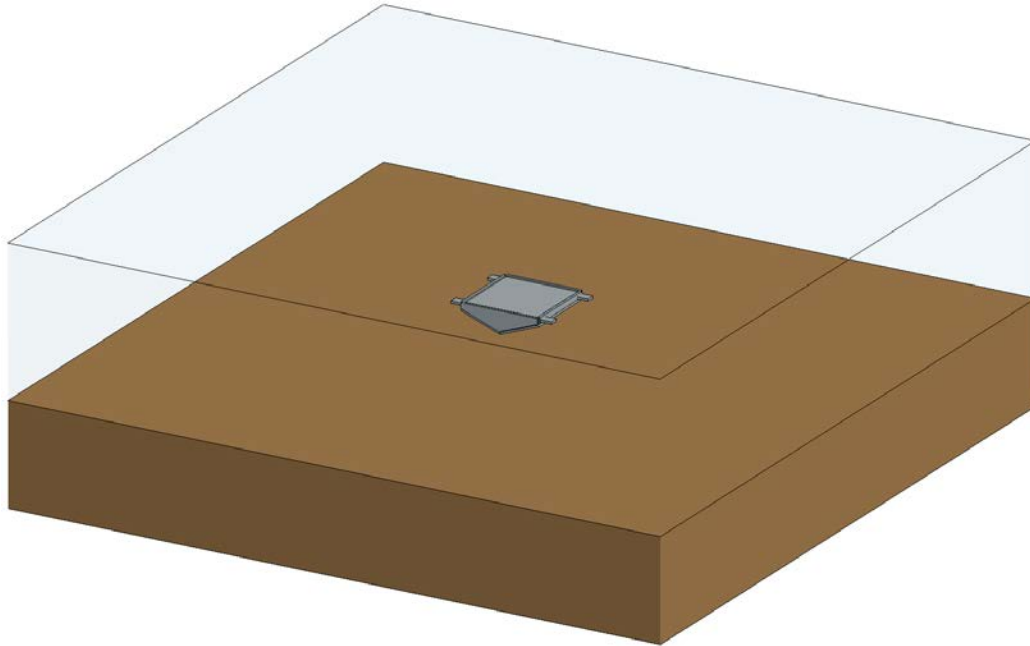


Fig. 16 ALE representation of the air, soil, and mine with the validated structural model

The material properties and equations of state for the soil were obtained from Cummins.⁷ The soil modeled in the reference is not the same soil used when testing the V-hull. However, there is empirical data to show that both soils under the same range conditions impart a similar amount of impulse per unit kg of TNT to the target. In this study, we make the assumption that the soil reacts the same way with cyclotrimethylene-trinitramine (C4) as it does with TNT, since the threats used in this test series were C4 and not TNT.

The ALE simulation was performed and the impulse imparted to the nonvalidated structural model was 1120 N-s. The impulse imparted to the validated structural model was 1098 N-s. The minimum, maximum, and average impulses calculated from the test data were 1047 N-s, 1138 N-s and 1097 N-s, respectively. Both impulses are within the range of impulse observed during testing and as such are deemed acceptable. It is unknown why the impulses don't match exactly between the validated and nonvalidated structural models. The difference could be related to the structural models themselves. For each model, impulse was estimated from LS-DYNA by plotting the linear momentum of the hull's center of mass as a function of time. Specifically, the linear momentum in the direction normal to the ground was plotted. The momentum calculation includes the rigid-body motion of the structure as well as the localized momentum as a result of deformation. Since the initial velocities of the hulls were zero in the simulations, the total impulse imparted to each hull is equal to the peak value of the corresponding linear momentum curve. At each time step, LS-DYNA recalculates the center of mass of

the structure and calculates its resultant momentum. When the structural model was validated, its overall stiffness changed. As a result, the deformation of the hull changes and the location of the center of mass at each time step can be different between the 2 models. These differences in stiffness can affect momentum and the estimated impulse to the target—resulting in the validated and nonvalidated models having somewhat different estimated impulses.

Having predicted reasonable impulses to the targets, attention is turned toward the predicted structural responses at the centers of the targets. Since the ALE model cannot be easily tuned to match an impulse observed during a test event, a more general approach is used to compare the model and test data. Figure 17 displays a “band” of displacements derived from the test data.

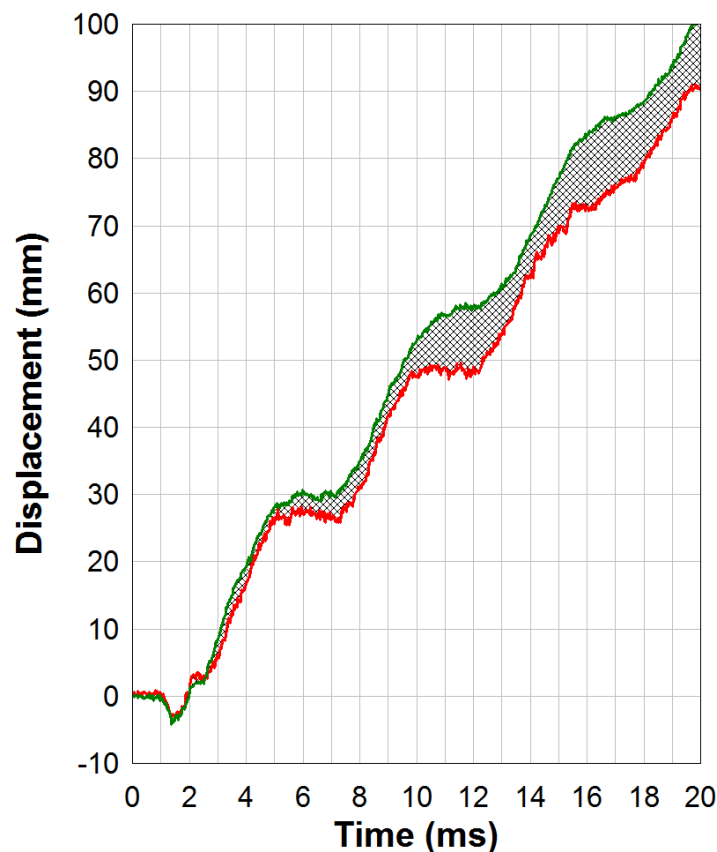


Fig. 17 Band of displacements derived from test data

Each of the thick curves (red and green) represents a structural response measured during testing at the center of the flat plate on the top of the hull. The upward trend in the plot represents the rigid-body displacement and the oscillation about the upward trend represents the localized structural displacement. The upper-most thick green line is the displacement obtained from the experiment for which the target experienced the largest impulse and the lower-most thick red line is the

displacement obtained from the experiment for which the target experienced the smallest impulse. This is consistent with the expectation that a larger impulse imparted to the structure would result in a larger rigid-body displacement and vice-versa. The shaded area in between the red and green curves represents the domain in which we would expect the measured structural displacement to fall if a repeat test were performed and the observed impulse fell within the range of those seen previously. The shaded area in between the 2 experimental curves also represents the theoretical domain in which the model prediction would fall if the impulse imparted to the modeled target is within range of those observed in testing and the modeled target is a good representation of the physical target.

Figure 18 compares the predicted displacement at the center of the nonvalidated model to the band of displacements obtained from the experimental data. The thick blue line in between the 2 experimental curves is the model prediction. Up to approximately 4 or 5 ms, the model prediction tracks relatively well with the experimental data but it is not within the shaded area as hoped.

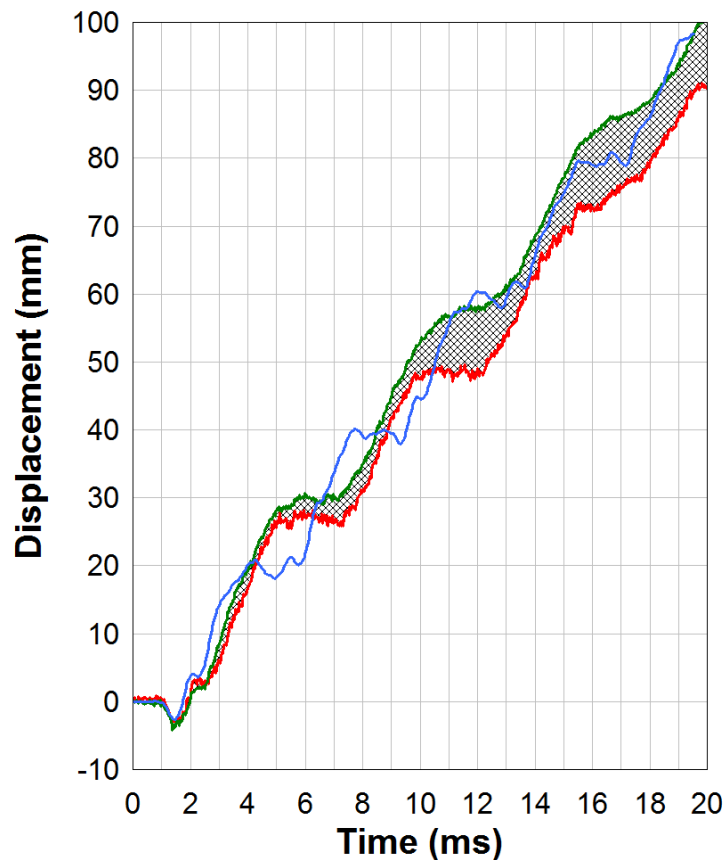


Fig. 18 Band of displacements derived from test data and model-predicted displacement using the nonvalidated structural model

Figure 19 compares the predicted displacement at the center of the validated model to the band of displacements obtained from the experimental data. Again the model prediction does not fall within the band of displacements, but subjectively the band and model prediction do appear to track one another more closely. No filters were applied to the experimental data or model predictions.

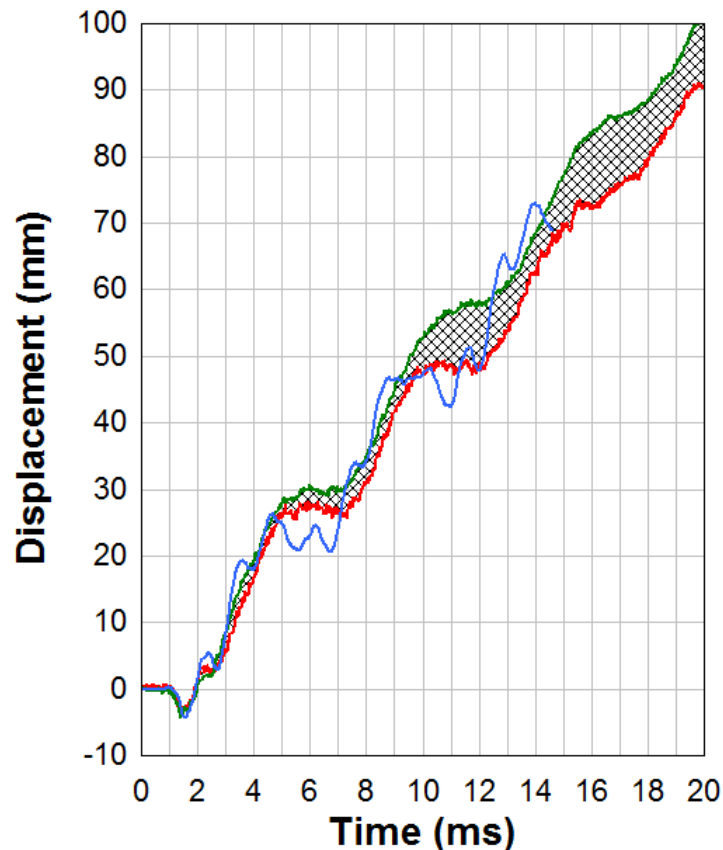


Fig. 19 Band of displacements derived from test data and model-predicted displacement using the validated structural model

As mentioned previously, it appears that the model data contains many more frequency components than that of the test data. It is possible to apply filters to the data to remove those higher frequencies but it does not greatly improve the model and test correlation. Figure 20 displays the model and test data for which a Society of Automotive Engineers (SAE) filter at 300 Hz was applied to the model-predicted structural response. The difference in the frequency components could be because damping is not included in the structural model. Damping may also affect the time delay between the peaks in the model and test structural responses.

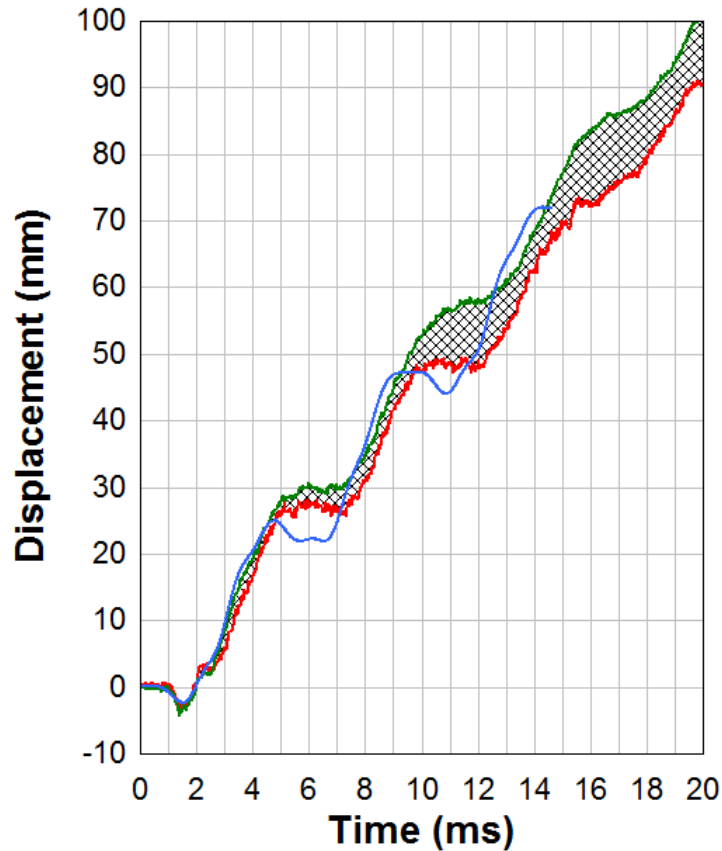


Fig. 20 Band of displacements derived from test data and model-predicted displacement using the validated structural model. The data from the structural model was filtered with an SAE filter at 300 Hz.

Once again the CORA tool was exercised on the test and model data to quantify the effect of model validation on the predictions. When the CORA tool was used to compare the prediction of displacement from the nonvalidated structural model to the test data, an overall rating of 0.926 was obtained. When the CORA tool was used to compare the prediction of displacement from the validated structural model to the test data, an overall rating of 0.907 was obtained. The model data was not filtered before calculating the CORA value. Although the CORA rating for the validated FE model is actually a little smaller than the rating for the nonvalidated model, both are similar and considered to be very good. The FE model predictions appear to be representative of the sample of test data points used for comparison. Table 4 compares the CORA scores calculated for each simulation prediction.

Table 4 Comparison of CORA scores for all model predictions

	Nonvalidated model	Validated model
ConWep	0.865	0.947
ALE	0.926	0.907

Overall, the CORA scores for all the model predictions were higher than a favorable rating. When the FE models were loaded with ConWep, the modal validation improved the prediction. When the FE models were loaded with ALE, the modal validation resulted in a lower CORA score. Detailed CORA reports are provided in the Appendix.

9. Conclusions

Modal analysis of the V-hull structure was successfully performed. The modal test setup, execution, and results obtained from modal tests were presented. The modal testing provided the model update parameters necessary to validate the structural finite element model. Changes that were made to the model as part of the validation process were documented. The disagreement between the mode shapes and natural frequencies was minimized by modeling the welds in the structure.

In general all models—whether validated, nonvalidated, loaded with ConWep or loaded with ALE—provided acceptable predictions of structural response. The CORA scores were all greater than 0.865. The modal-based validation of the finite element model improved the prediction of the response of the structure subjected to a ConWep-based simulation of the mine blast. The modal-based validation worsened the prediction of the response of the structure subjected to an ALE simulation of the mine blast, but only by a small amount.

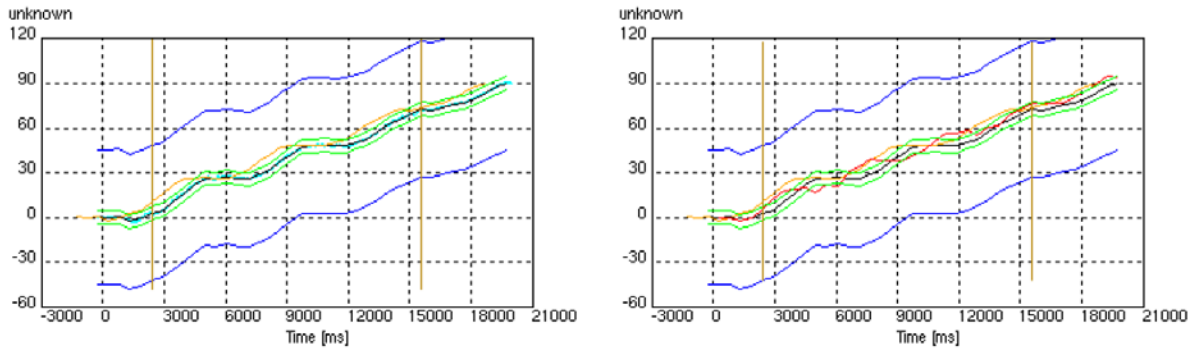
10. References

1. ATEC Pamphlet 73-21: Modeling and simulation verification, validation and accreditation methodology. Alexandria (VA): Army Test and Evaluation Command (US); 2007 Apr 13.
2. DA Pamphlet 5-11: Verification, validation and accreditation of Army models and simulations. Washington (DC): Department of the Army (US); 1999 Sep 30.
3. Huang X, Cheeseman B, Yen C. Blast dynamic responses of V-shaped hulls. Aberdeen Proving Ground (MD): Army Research Laboratory (US); 2007 Oct. Report No.: ARL-TR-4293.
4. Neuberger A, Peles S, Rittel D. Scaling the response of circular plates subjected to large and close-range spherical explosions. Part II: buried charges. *Int J Impact Eng.* 2007;34(5):874–882.
5. Ma Z, Jiang D, Liu Y, Raju B, Bryzik W. Function-oriented material design for innovative composite structures against land explosions. Ann Arbor (MI): The University of Michigan. 2006 Nov 1.
6. Wang J. Simulation of landmine explosion using LS-DYNA3D software: benchmark work of simulation of explosion in soil and air. Fishermans Bend, Victoria (Australia): Australian Department of Defence; Defence Science & Technology Organisation, Aeronautical and Maritime Research Laboratory; 2001 June. Report No.: DSTO-TR-1168.
7. Cummins C. Modeling brown clayey sand in LS-DYNA with an analytical method for soil state initialization. Aberdeen Proving Ground (MD): Army Research Laboratory (US); 2014. Report No.: ARL-TR-6830.
8. Barker C, Howle D, Holdren T, Koch J, Ciappi R. Results and analysis from mine impulse experiments using stereo-digital image correlation. Aberdeen Proving Ground (MD): Army Research Laboratory (US); 2012 May. Report No.: ARL-RP-0370.
9. Howle D, Ciappi R. Predicting the responses of simple structures subjected to mine blast loading. Aberdeen Proving Ground (MD): Army Research Laboratory (US); 2007 Sep. Report No.: ARL-TR-6145.
10. Berman M. Modal analysis of the prototype heavy composite hull (HCH). Aberdeen Proving Ground (MD): Army Research Laboratory (US); 1998 Feb. Report No.: ARL-MR-387.

11. Berman M. Modal analysis of the M113 armored personnel carrier metallic hull and composite hull. Aberdeen Proving Ground (MD): Army Research Laboratory (US); 1995 Aug. Report No.: ARL-MR-246.
12. Berman M, Li T. Modal analysis of Bradley fighting vehicle (BFV): prototype composite hull and production metallic hull. Aberdeen Proving Ground (MD): Army Research Laboratory (US); 1994 June. Report No.: ARL-TR-445.
13. Benesch B. Evaluation of UBM ALE loading: simulation comparison to sandbox V-hull tests. Aberdeen Proving Ground (MD): Army Research Laboratory (US); 2017 Aug. Report No.: ARL-CR-0818.
14. Gray G, Chen S, Wright W, Lopez M. Constitutive equations for annealed metals under compression at high strain rates and temperatures. Los Alamos (NM): Los Alamos National Laboratories; 1994 Jan. Report No.: LA-12669-MS.
15. UFC 3-340-01 Design and analysis of hardened structures to conventional weapons effects. Washington (DC): Army Corps of Engineers (US); 2002 June.
16. ConWep. Protective Design Center. United States Army Corps of Engineers; 2017 [accessed 2017 Nov 17]. <https://pdc.usace.army.mil/software/conwep>.
17. Williams K, McClennan S. A numerical analysis of mine blast effects on simplified target geometries: validation of loading models. Val-Bélair, Quebec (Canada): Defence R&D Canada – Valcartier; 2002. Report No.: DRDC-VALCARTIER-TM-2002-260.
18. Baranowski P, Malachowski J, Neizgoda T. Numerical analysis of vehicle suspension system response subjected to blast wave. Appl Mech Mater. 2011;82:728–733.
19. Gehre C, Gades H, Wernicke P. Objective rating of signals using test and simulation responses. Proceedings of the 21st (ESV) International Technical Conference on the Enhanced Safety of Vehicles; 2009 June 15–18; Stuttgart, Germany. National Highway Traffic Safety Administration; 2009.
20. Baker W, Untaroiu C, Chowdhury M. Development of a finite element model of the WIAMan lower extremity to investigate under-body blast loads. 14th International LS-DYNA Users Conference; 2016 June 12–14; Detroit, MI. Aberdeen Proving Ground (MD): Army Research Laboratory (US); 2016.

Appendix. Detailed CORA Reports

Detailed CORA Report for Nonvalidated Hull with ConWep Loading:

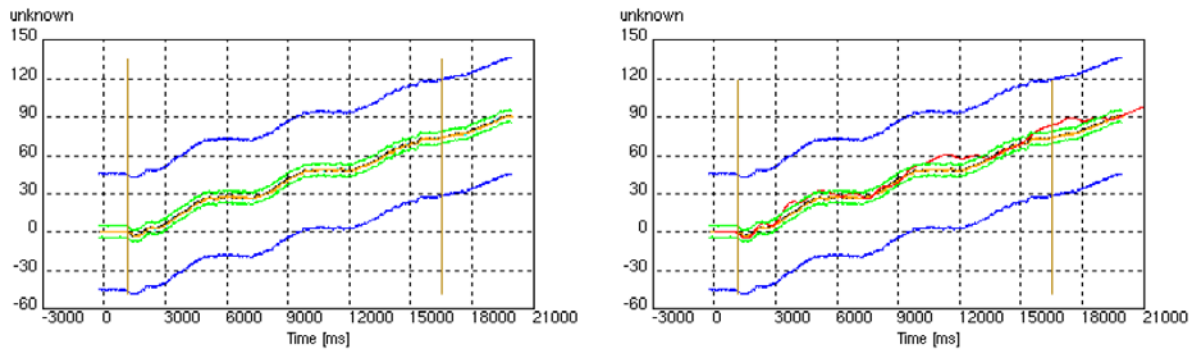


<p>test_01</p> <p>test_02</p>	<p>Average of experiments</p> <p>cross-correlation reference</p> <p>dyna</p> <p>Limits Outer corridor</p> <p>Limits inner corridor</p>
-------------------------------	--

Method	Name	Rating	Weight			
1	Corridor Method	0.933	0.50			
2	Correlation Method	0.798	0.50			
				Value	Rating	Weight
	Cross correlation function			0.994	0.970	0.50
	Size			0.888	0.888	0.250
	Phase shift	1053.5	0.364	0.250		
3	Combination of 1 and 2	0.865	-			

Parameters:	Evaluation Intervall:	2389.7 - 15558.8
Method 1:	Max. half width of inner corridor:	0.050
	Max. half width of outer corridor:	0.50
	Corridor curve file:	
	Reference value:	90.627
Method 2:	Transition exponent:	2
	Limits for phase shift:	131.7 - 1580.3
	Rating exponents (shape, size, phase):	10, 1, 1

Detailed CORA Report for Validated Hull with ConWep Loading:

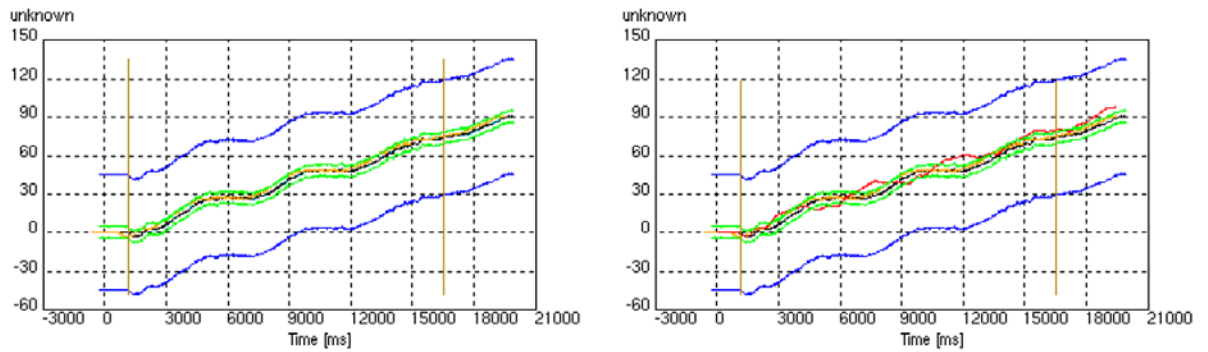


test_01	Average of experiments
test_02	cross-correlation reference
	dyna
	Limits Outer corridor
	Limits inner corridor

Method	Name	Rating	Weight			
1	Corridor Method	0.944	0.50			
2	Correlation Method		0.951	0.50		
		Value			Rating	Weight
	Cross correlation function	0.996			0.982	0.50
	Size	0.840			0.840	0.250
	Phase shift	-90.2	1.0	0.250		
3	Combination of 1 and 2	0.947	-			

Parameters:	Evaluation Interval:	1164.9 - 16492.8
Method 1:	Max. half width of inner corridor:	0.050
	Max. half width of outer corridor:	0.50
	Corridor curve file:	
	Reference value:	91.063
	Transition exponent:	2
Method 2:	Limits for phase shift:	153.3 - 1839.4
	Rating exponents (shape, size, phase):	10, 1, 1

Detailed CORA Report for Nonvalidated Hull with ALE Loading:

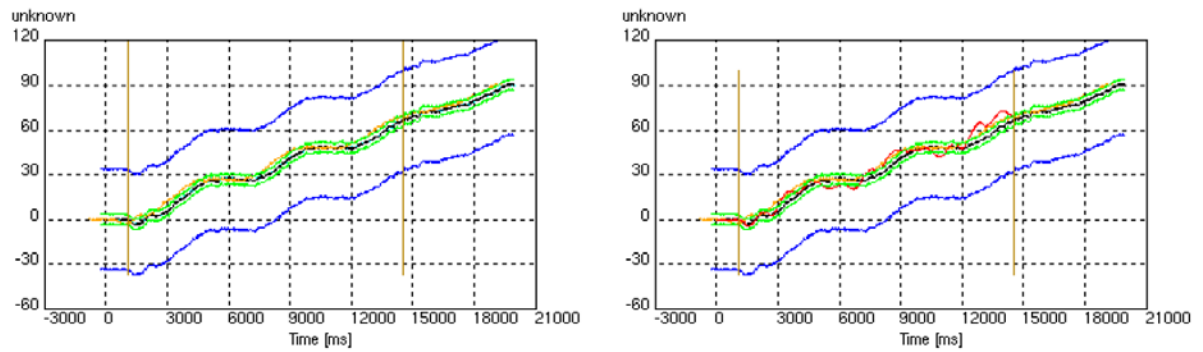


test_01	Average of experiments
test_02	cross-correlation reference
	dyna
	Limits Outer corridor
	Limits inner corridor

Method	Name	Rating	Weight			
1	Corridor Method	0.922	0.50			
2	Correlation Method	0.930	0.50			
				Value	Rating	Weight
	Cross correlation function			0.994	0.972	0.50
	Size			0.918	0.918	0.250
	Phase shift	390.8	0.859	0.250		
3	Combination of 1 and 2	0.926	-			

Parameters:	Evaluation Intervall:	1165.5 - 16497.1
Method 1:	Max. half width of inner corridor:	0.050
	Max. half width of outer corridor:	0.50
	Corridor curve file:	
	Reference value:	89.888
	Transition exponent:	2
Method 2:	Limits for phase shift:	153.3 - 1839.8
	Rating exponents (shape, size, phase):	10, 1, 1

Detailed CORA Report for Validated Hull with ALE Loading:



test_01	Average of experiments
test_02	cross-correlation reference
	dyna
	Limits Outer corridor
	Limits inner corridor

Method	Name	Rating	Weight			
1	Corridor Method	0.90	0.50			
2	Correlation Method	0.914	0.50			
				Value	Rating	Weight
	Cross correlation function			0.996	0.979	0.50
	Size			0.994	0.994	0.250
	Phase shift	571.1	0.705	0.250		
3	Combination of 1 and 2	0.907	-			

Parameters:	Evaluation Intervall:	1104.9 - 14570.0
Method 1:	Max. half width of inner corridor:	0.050
	Max. half width of outer corridor:	0.50
	Corridor curve file:	
	Reference value:	67.173
Method 2:	Transition exponent:	2
	Limits for phase shift:	134.7 - 1615.8
	Rating exponents (shape, size, phase):	10, 1, 1

INTENTIONALLY LEFT BLANK.

List of Symbols, Abbreviations, and Acronyms

ALC	Adelphi Laboratory Center
ALE	arbitrary Lagrangian-Eulerian
AMSAA	Army Material Systems Analysis Activity
APG	Aberdeen Proving Ground
ARL	US Army Research Laboratory
ATEC	US Army Test and Evaluation Command
C4	cyclotrimethylene-trinitramine
CORA	correlation and analysis
ERDC	US Army Engineer Research and Development Center
FE	finite element
MAC	modal assurance criteria
SAE	Society of Automotive Engineers
SDIC	stereo-digital image correlation
SLAD	Survivability/Lethality Analysis Directorate
T&E	Test and Evaluation
TARDEC	Tank Automotive Research, Development and Engineering Center
TNT	trinitrotoluene or 2,4,6-trinitrotoluene
UBM	Under-body Blast Methodology
VV&A	verification, validation, and accreditation
WMRD	Weapons and Materials Research Directorate

1 DEFENSE TECHNICAL
(PDF) INFORMATION CTR
DTIC OCA

2 DIR ARL
(PDF) IMAL HRA
RECORDS MGMT
RDRL DCL
TECH LIB

1 GOVT PRINTG OFC
(PDF) A MALHOTRA

2 OAK RIDGE INST FOR SCI AND EDUCATION
(PDF) JE PRITCHETT
R SORENSON

2 DIR ARL
(PDF) RDRL SLB E
D HOWLE
D KRAYTERMAN